AD-A070 798 NORTHWESTERN UNIV EVANSTON IL DEPT OF MATERIALS SCIENCE F/G 11/6
RESIDUAL STRESSES IN GROUND STEELS.(U)
JUN 79 H DOELLE, J B COHEN N00014-75-C-0580
UNCLASSIFIED TR-24 NL

1 OF 1
AD
A070798

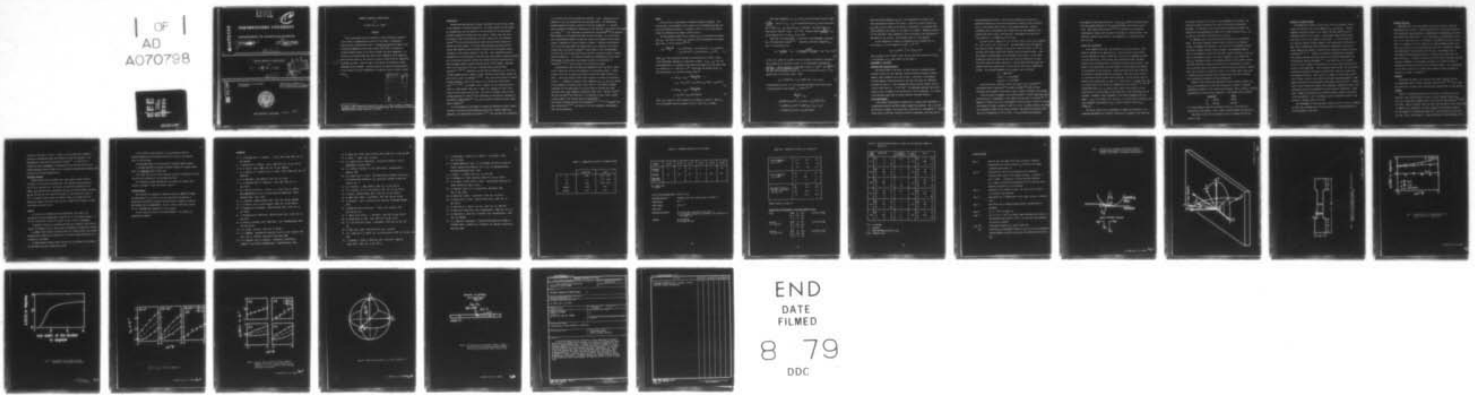

END
DATE
FILMED
8 79
DDC

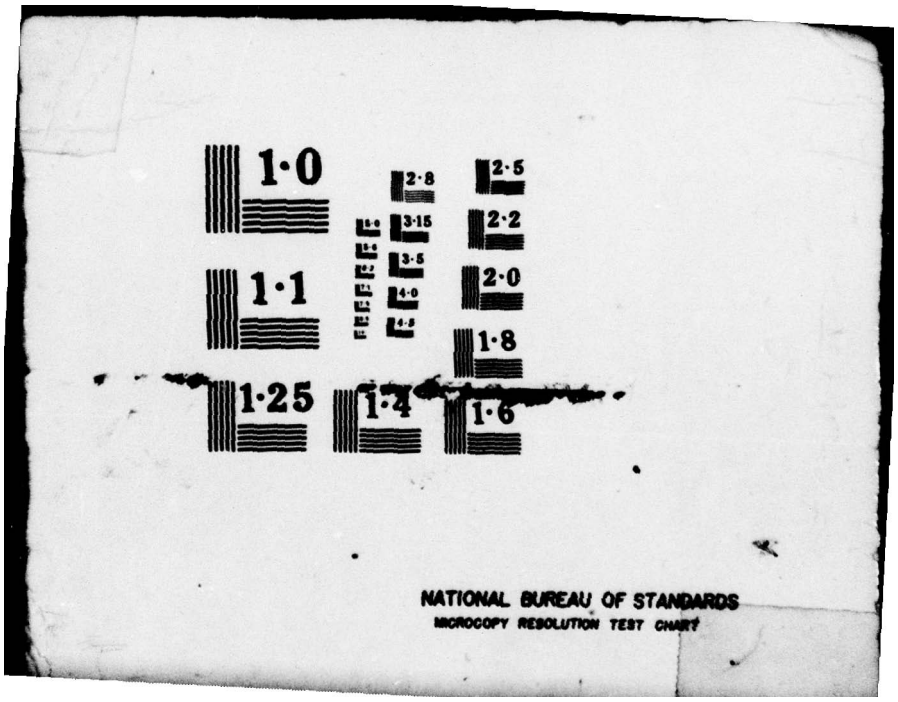
1·0
1·1
1·25
1·4
1·6
1·8
2·0
2·2
2·5
2·8
3·15
3·5
4·0
NATIONAL BUREAU OF STANDARDS
MICROCOPY RESOLUTION TEST CHART

NORTHWESTERN UNIVERSITY

DEPARTMENT OF MATERIALS SCIENCE

(9) Technical Report No. 24
(13) June 1979
(11)

(15) Office of Naval Research
Contract N00014-75-C-0580
NR 031-733

(14) TR-24

(6) RESIDUAL STRESSES IN GROUND STEELS.

by

(10) H. E. Dolle and J. B. Cohen

(12) 33 p.

EVANSTON, ILLINOIS 260 810

RESIDUAL STRESSES IN GROUND STEELS

by

H. Dölle and J. B. Cohen*

ABSTRACT

A new X-ray method for the evaluation of three dimensional (residual) stress states is demonstrated by studies of the effect of grinding on Armco-iron and a medium carbon steel. Although the penetration depth of the Cr-radiation employed in this study is only 5 μm, there is evidence of residual stresses normal to the surface (normal and shear components). In the past it has been assumed that these stress components can be neglected. Shear stresses normal to the surface are small in Armco iron, but significant (± 60 MPa) in steel. From the sign of the shears, the direction of final grinding can be determined. Cooling decreases the tensile stresses parallel to the surface in steel; surprisingly, the opposite result is found in Armco-iron.

*H. Dolle is Post-Doctoral Visiting Scholar and J. B. Cohen is Frank C. Engelhart Professor, Dept. of Materials Science and Engineering, The Technological Institute, Northwestern University, Evanston, IL. 60201.

INTRODUCTION

During machining (milling, turning or grinding) the near-surface region of the workpiece is deformed plastically. As volume elements in this region are extended when the tool passes by, the constraints of the bulk should introduce compressive stresses near the surface. Indeed, this does occur for shallow, slow, well-lubricated cuts with a sharp tool. But extensive studies[1-12] of the stress pattern have shown that the actual situation is usually much more complex: If strong work hardening occurs only near the surface this produces tensile residual stresses, due to the greater elastic relaxation of this region compared to the bulk. Local compressive plastic deformation due to the pressure by the tool will cause tensile residual stresses, and, if the sum of external stresses and residual stresses exceed the local yield strength, plastic recovery will take place in this region. Even when there is no cross-feed of the tool, a biaxial stress state has been observed[3, 8, 10, 12]. Heating due to the lack of lubrication or, a dull tool or high downfeed produces tensile stresses because locally heated regions are upset by the cooler surroundings[4, 8, 12]. Thus, the stress pattern is altered by many parameters, such as the depth of cut, cooling and cutting direction[2, 3, 7, 10-12]. For example, after a deeper cut, the stress pattern extends to a depth greater than after a light cut, although the value of the stress near the surface can be lower. The level of residual stress is also strongly affected by carbon,[13] which influences the microplastic behaviour of the material significantly.[14] Also, these residual stresses can affect dimensional stability.[15]

It is the purpose of this paper to examine the influence of some of these variables on stresses after grinding Armco-iron and a medium carbon steel, employing a new experimental X-ray method [16, 17] that provides more information

on the stress-state than was heretofore available. Also, a comparison of the behaviour of two such materials has not been made before. The experimental methods employed in previous studies fall into two categories: 1. Stresses were calculated from mechanical deflection of the work-piece when layers were removed by etching.[1-5] 2. The traditional non-destructive X-ray method[18-20] was employed which averages over the penetration depth of the X-ray beam. It is more selective than mechanical methods, because the strains are averaged over only those grains or subgrains of a phase oriented to diffract. Because of the selectivity of the X-ray measurement the stresses have to be calculated from lattice strains with X-ray elastic constants[17], which depend on the crystallographic direction $\langle hk\ell \rangle$ and the polycrystalline properties (coupling of grains, texture, plastic deformation). The stresses evaluated are representative of the volume diffracting, and even when no macroscopic stresses can be detected by deflection[15, 21, 22] local stresses can be detected by X-rays.

During grinding there are normal and tangential forces (F_n and F_t respectively) between the tool and the workpiece[5] as illustrated in Fig. 1. These external forces can be resolved into shear stresses and normal stresses, as shown. (The axial system to which these stresses are related is illustrated in Fig. 2.) Although the residual stress components σ_{33}, σ_{13} (and σ_{23}) induced on the workpiece by external forces F must vanish at the surface, averages associated with the penetration of the X-ray beam can include such terms, especially when a high tangential deformation takes place. Recently, Peiter[23] and Dölle and Hauk[16] have shown that it is possible to detect these residual stresses normal to the surface from X-ray measurements.
Such effects have been observed after grinding[10, 11, 24, 25, 26] turning[12] and after surface wear.[27, 28] This paper is the first systematic investigation with this new procedure.

THEORY

In what follows, right-handed co-ordinate systems are employed. The direction $\underline{P}_1$ in the specimen's axial system is in the grinding direction and $\underline{P}_2$ is the transverse direction. A positive ψ tilt is a tilt of the surface toward the diffracted X-ray beam as shown in Fig. 2.

The relationship between lattice strains $\epsilon'_{\Phi\psi}$ in the direction of measurement, $\underline{L}_3$, and lattice strains ϵ_{ij}, related to the co-ordinates of the sample ($\underline{P}_1$ in Fig. 2) can be written as[17, 29]:

$$\epsilon'_{\Phi\psi} = \frac{d_{\Phi\psi} - d_o}{d_o} = \epsilon_{11}\cdot\cos^2\Phi\cdot\sin^2\psi + \epsilon_{12}\cdot\sin 2\Phi\cdot\sin^2\psi + \epsilon_{13}\cdot\cos\Phi\cdot\sin 2\psi + \epsilon_{22}\cdot\sin^2\Phi\cdot\sin^2\psi + \epsilon_{23}\cdot\sin\Phi\cdot\sin 2\psi + \epsilon_{33}\cdot\cos^2\psi, \quad [1]$$

where $d_{\Phi\psi}$ is the interplanar spacing for the direction $\Phi\psi$ in Fig. 2 and d_o is the interplanar spacing of a stress-free standard. If ϵ_{13}, $\epsilon_{23} \neq 0$, the relationship (Eq. 1) is different for positive and negative ψ tilts which leads to a "split" in d vs. $\sin^2\psi$ for $\pm\psi$.[24] Introducing the average strain, a_1, and the deviation, a_2, from this average strain;[16]

$$a_1 = \tfrac{1}{2}[\epsilon_{\Phi\psi+} + \epsilon_{\Phi\psi-}] = \frac{d_{\Phi\psi+} + d_{\Phi\psi-}}{2d_o} - 1,$$

$$= \epsilon_{33} + [\epsilon_{11}\cdot\cos^2\Phi + \epsilon_{12}\cdot\sin 2\Phi + \epsilon_{22}\cdot\sin^2\Phi - \epsilon_{33}]\cdot\sin^2\psi. \quad [2]$$

$$a_2 = \tfrac{1}{2}[\epsilon_{\Phi\psi+} - \epsilon_{\Phi\psi-}] = \frac{d_{\Phi\psi+} - d_{\Phi\psi-}}{2d_o},$$

$$= [\epsilon_{13}\cdot\cos\Phi + \epsilon_{23}\cdot\sin\Phi]\cdot\sin|2\psi|. \quad [3]$$

Here, a_1 is linear vs. $\sin^2\psi$, whereas a_2 is linear vs. $\sin|2\psi|$. Thus, ϵ_{33} can be determined from the intercept of a_1 vs. $\sin^2\psi$ if d_o is known.

The tensor components ϵ_{11}, ϵ_{12}, and ϵ_{22} can be evaluated from the slope, $(\frac{\partial a_1}{\partial \sin^2 \psi})$. For $\Phi = 0$, $\epsilon_{11} - \epsilon_{33}$ is obtained and hence ϵ_{11} can be calculated. For $\Phi = 90^\circ$; $\epsilon_{22} - \epsilon_{33}$ (and hence ϵ_{22}) is obtained. The shear strain ϵ_{12} then results from this slope at $\Phi = 45^\circ$. From the slopes $(\frac{\partial a_2}{\partial \sin|2\psi|})$, ϵ_{13} can be deduced for $\Phi = 0$ and ϵ_{23} for $\Phi = 90^\circ$.

Since the X -ray measurement is selective, crystallographic anisotropy has to be taken into account.[16, 17] Therefore, the stress components σ_{ij} have to be calculated from:

$$\sigma_{ij} = \frac{1}{\frac{1}{2}s_2(hk\ell)} \cdot [\epsilon_{ij} - \delta_{ij} \frac{s_1(hk\ell)}{\frac{1}{2}s_2(hk\ell) + 3 \cdot s_1(hk\ell)} \cdot (\epsilon_{11} + \epsilon_{22} + \epsilon_{33})]. \qquad [4]$$

In eqn. [4] $s_1(hk\ell)$ and $\frac{1}{2}s_2(hk\ell)$ are the isotropic X-ray elastic constants,[17] which depend on the reflection chosen for the measurement of interplanar spacings. (These constants are sometimes written as $(-\frac{\nu}{E})^{hk\ell}$ and $(\frac{1+\nu}{E})^{hk\ell}$.) The term δ_{ij} is the Kronecker delta.
The axes of the principal stresses, H_i, can be calculated by means of a diagonalization of the stress tensor. When:

$$\epsilon_{ij} = \tfrac{1}{2}s_2(hk\ell) \cdot \sigma_{ij} + \delta_{ij} \cdot s_1(hk\ell) \cdot [\sigma_{11} + \sigma_{22} + \sigma_{33}]; \qquad [5]$$

is substituted into eqn. [1], the relationship between the lattice strain in the direction $\Phi\psi$ and stresses σ_{ij} results:[16, 17]

$$\frac{d_{\Phi\psi} - d_o}{d_o} = \epsilon_{\Phi\psi} = \qquad [6]$$

$$= \tfrac{1}{2}s_2(hk\ell) \cdot [\sigma_{11} \cdot \cos^2\Phi + \sigma_{12} \cdot \sin 2\Phi + \sigma_{22} \cdot \sin^2\Phi] \cdot \sin^2\psi +$$

$$+ \tfrac{1}{2}s_2(hk\ell) \cdot \sigma_{33} \cdot \cos^2\psi + s_1(hk\ell)[\sigma_{11} + \sigma_{22} + \sigma_{33}] +$$

$$+ \tfrac{1}{2}s_2(hk\ell) \cdot [\sigma_{13} \cdot \cos\Phi + \sigma_{23} \cdot \sin\Phi] \cdot \sin 2\psi,$$

where the stress components σ_{ij} are to be interpreted as average values over the penetration depth of the X-rays. Since the residual stresses σ_{13}, σ_{23} (and σ_{33}) must vanish in the surface, ψ-splitting is only possible when stress gradients with respect to the depth z are present. Employing equation [6] the individual stress components could be obtained in the same manner as described for the strains. In this paper, Eqns. 2-4 were employed.

As the absorption of X-rays is accounted for by an exponential law, the average σ_{ij} over the penetration depth τ is[17, 30]:

$$\sigma_{ij} \approx \sigma_{ij}(z=0) + \int_0^D \exp\left[-\frac{z}{\tau}\right] \cdot g_{ij}(z) \cdot dz, \qquad [7]$$

where $\sigma_{ij}(z=0)$ is the surface stress, D is the total beam penetration and g_{ij} is the gradient in σ_{ij} with respect to the depth, z.

EXPERIMENTAL PROCEDURES

Materials and Grinding Methods

Hot-rolled sheets (2 mm thick) of Armco iron and a normalized plain (medium) carbon steel were employed; chemical analyses are given in Table I. Samples, whose dimensions are shown in Fig. 3, were held to the grinding bed with magnetic chucks and ground on one side only under the conditions described in Table II. After grinding and removal from the chucks, the curvatures varied from 1.5 - 3.2 10^{-4} mm^{-1}. The grinding conditions were deliberately severe to emphasize the differences in the two materials. As a result, those specimens which were not cooled exhibited burnished surfaces.

X-ray Measurements

A G.E. XRD-5 diffractometer equipped with a quarter-circle goniometer, a scintillation detector and pulse height analyzer were employed. The ψ tilt and 2θ rotation to examine the 211 peak were controlled by a minicomputer.[31] The intensities across a peak were corrected on-line for absorption, dead time and the

Lorentz-polarization factor. The code also determined the location of a diffraction peak and its associated interplanar spacing "d" from a parabolic fit of 7 data points within 15 pct of the maximum intensity. Circular collimators with 1 mm diameters and a length of 95 mm were employed in the incident beam and in front of the detector. Measurements were made with CrK_α radiation (λ = 0.228965 nm; 50 kV 15 mA).

For each of the Φ angles of 0°, 45° and 90°, eleven ψ tilts were examined: 0°, $\pm 18^\circ$, $\pm 26^\circ$, $\pm 33^\circ$, $\pm 39^\circ$, $\pm 45^\circ$. The measurements were each repeated four times to obtain estimates of the errors in the "d" values ($\simeq 10^{-5}$ nm) and hence the stresses (which were obtained from the average strains). With this system, all measurements on one specimen took 24 hours. As the reproducibility of data was high this time could easily be reduced to 2-3 hours with fewer peaks and without repetitions. Several peaks from the ground and unground faces were examined and it was found that there was no appreciable texture. The constants employed in data analysis were as follows:

$$d_o = .28665 \text{ nm}^{32}$$

$$s_1(211) = -1.25 \cdot 10^{-6} \text{MPa}^{-1}$$

$$\tfrac{1}{2}s_2(211) = 5.77 \cdot 10^{-6} \text{MPa}^{-1}.$$

The X-ray elastic constants $s_1(211)$ and $\frac{1}{2}s_2(211)$ were calculated[17,33] from single-crystal compliances[34] according to Kröner's[35] theory of bulk elasticity which assumes an anisotropic crystal coupled to isotropic surroundings.

Care was taken in alignment of the diffractometer to avoid ψ-splitting which can occur due to a displacement of the sample from the axes of ψ-rotation.[36, 37] Examples of effects due to this displacement are shown in Fig. 4 which was obtained with sieved Cr filings, annealed at 450°C for 3 hrs. to remove stresses, and painted on a specimen's surface in an acetone solution. The sample was displaced until there was no dependence of "d" vs $\sin^2\psi$. In this position the goniometer

was aligned and the powder was removed. The K_{α_1}-K_{α_2} doublet resolution varied from the annealed materials to the ground specimens, and with the various tilts. This affects peak location.[37, 38] A correction was obtained by simulating the doublet with two Gaussian functions of various widths. The resultant variation shown in Fig. 5 was employed as a correction to each peak location.

RESULTS AND DISCUSSION

As an example of the data, the variation in lattice strain vs. $\sin^2\psi$ found for specimen C5 is shown in Fig. 6. The strain and stress-tensors for this specimen are given in Table III, as well as the principal stresses and their directions. These results show clearly how readily the shear stresses can be determined from ψ splitting, even when they are small. Also shown are the results when the older methods of stress analysis are applied in the presence of this splitting. Clearly previous data in the literature on stresses in machining should be re-examined. The solid curves in Fig. 6 are calculated from the stress-tensors using Eqn. [6]; the dotted curve represents the average strain a_1, Eqn. [2]. Since this is a straight line, this is a further proof that texture was unimportant in this study.[17, 24, 39, 40] As mentioned above, σ_{13}, σ_{23} and σ_{33} must vanish at the surface, and the listed values are the averages of the penetration of the X-ray beam into the specimen. Assuming a linear dependence of the stress-components with the depth, z, ($\sigma_{ij} = k \cdot z$ in Eqn. [7]), and that $\tau \approx 5$ μm for the 211-reflection and CrK_α-radiation, the gradient for σ_{13} is about 12 MPa μm^{-1} and for σ_{33}, 18 MPa μm^{-1}.

The stress tensors for all specimens are summarized in Table IV. By repeating measurements at different locations on a specimen it was found that

the highest variation in the normal stress-components was $\pm$ 60 MPa. The variation of shear stresses was less than the accuracy of measurement ($\pm$ 8 MPa). By solving for the stresses with the annealed Cr-powder, the precision in the measurement was found to be 15 MPa or better for σ_{11}, σ_{12}, σ_{22} and σ_{33}, and better than 8 MPa for σ_{13} and σ_{23}.

All specimens had a curvature with the ends bent up to the grinding wheel. The tensile residual stresses listed in Table IV are therefore acting to straighten the specimens. But there was no relationship between the surface residual stresses and the bending. The unmachined opposite sides of the samples A1 and C1 had only small residual stresses σ_{11} and σ_{22}, and no ψ-splitting was found. The stress component σ_{11} was always less than σ_{22}, sometimes positive and sometimes negative. These results clearly show that the entire residual stress pattern is concentrated in a region near the ground surface and cannot be calculated from the curvature. Furthermore, these stresses are opposite in sign to the stresses which would cause a uniform macroscopic bending, which indicates that they did not develop after removing the workpiece from the grinding bed.

Samples A5 and C5 which had appreciable tensile residual stresses (σ_{11} and σ_{22}) from grinding were then bent plastically to produce a curvature approximately opposite to that found after grinding. Both σ_{11} and σ_{22} decreased considerably but did not become compressive. The changes were as follows:

	Armco-iron	Steel
σ_{11}	-230 MPa	-320 MPa
σ_{22}	-140 MPa	-230 MPa

It is interesting to note that the shear stress σ_{13} in the steel was unaffected by this bending (and no shear stress developed in Amrco-iron).

The effect of each of the variables that were examined will be discussed in turn.

Influence of Carbon Content

An examination of Table IV reveals that, with one exception, tensile values were found for the stress components σ_{11}, σ_{22} and σ_{33}. The σ_{33} component, which must vanish at the surface, was much smaller than the components parallel to the surface. Surprisingly high tensile stresses were found in four of the samples of Armco-iron. It is well known that the resultant residual stresses depend on the distribution of dislocations. Their final configuration and the microplastic behaviour of iron and its alloys depend on the amount of carbon and the temperature during the plastic deformation.[13, 14, 41] Studies on dislocation configurations associated with residual stresses have been carried out by Kolb and Macherauch[42] and by Bollenrath, Hauk and Weidemann.[43] It was found that, in low carbon steel or in iron, tangles of dislocations occur after plastic tensile deformation at room temperature. With increasing carbon content, the dislocations become more uniformly distributed in glide planes, pinned by carbon atoms and cementite particles. When clusters or tangles of dislocations result[43] small residual stresses occur within the coherent scattering regions; a homogeneous distribution of dislocations yields high residual stresses. Perhaps, Armco iron has dislocation tangles after grinding; a comparative study of the dislocation structure in grinding and tension would be interesting. Three other reasons are possible for the observed tensile stresses as mentioned in the introduction: heat development, surface hardening and plastic compression of surface layers by the tool.

The development of the large shear residual stresses in steel as compared to Armco iron is perhaps due to the restrictions to dislocation motion by the second phase in the steel.

Grinding Direction

Specimens A1-A3, C1-C3 were ground in only one direction, along the positive $\underline{P}_1$ axis, see Fig. 2, whereas specimens A4-A6 and C4-C6 were ground in two-directions ($\pm \underline{P}_1$ direction), finishing with the negative $\underline{P}_1$ direction. Some results are shown in Fig. 7. Note that when σ_{13} is positive the curve for $\psi > 0$ is above that for $\psi < 0$ and when it is negative the curves reverse. Thus it is possible to tell the direction of final grinding from such data. Since σ_{23} is small it can be concluded that there was no significant tangential deformation in the transverse direction $\underline{P}_2$. The primary effect of reversing the final grinding direction is to reverse the direction of the shear stress σ_{13}. It should be noted also that the sign of the shear residual stresses is opposite to the grinding direction (as it should be since it represents the effect of the bulk on the sheared surface). It is interesting to note that no (or only very small) shear residual stresses developed in Armco-iron, see Fig. 7 and Table IV.

Downfeed

Increasing the depth of cut increases the normal stresses, but does not appreciably affect the shear stresses, Krause et al.[27, 28, 40] have found that these shear stresses reach limited values characteristic of each material.

Cooling

There is a surprising difference in the effect of cooling on the two materials. Since local heating can lead to tensile residual stresses (σ_{11} and σ_{22}), cooling should suppress these, as has in fact been observed[3-5, 7, 8, 12] for steel. This is certainly also the effect with the steel in this study (which is similar in its composition to steels examined in the previous studies). But the opposite is observed with Armco-iron. Two explanations can be given for this. First, there might be a larger difference in work hardening of the

surface of iron than for steel. Second, a stress relief due to dynamical recovery of dislocations under the influence of heat can take place. The mechanisms for such processes have been reviewed.[14] It could be concluded that less rearrangement of dislocation occurs in steel than in iron during machining without coolant; this is certainly indicated by the higher shear stresses in the steel mentioned above.

Principal Stresses

These coincide with the sample axial system when the shear stresses are small, as is the case for Armco-iron. The maximum deviation observed was 6° in φ_1 (see Fig. 8a). For steels, the transverse direction of the sample, $\underline{P}_2$, coincide with one principal axis, $\underline{H}_2$; but the principal directions $\underline{H}_1$, $\underline{H}_3$, see Fig. 8b, were tilted with respect to the surface by as much as 13°. It should be kept in mind, that these values are averages over the penetration depth of the X-ray beam, and that there will be regions in which much higher deviations occur.

SUMMARY

1) A new X-ray technique has been demonstrated, that permits the evaluation of the three dimensional stress-state in near surface regions. It will be of particular interest in studies of wear as well as machining.

2) Residual stresses in a ground work piece are confined to near surface layers; the bending of such a piece cannot be employed to estimate the stresses.

3) Higher shear residual stresses develop in a medium carbon steel during grinding than in Armco iron, probably due to the more random dislocation distribution in the former.

4) High tensile residual normal stresses due to grinding can be produced in both Armco iron and a medium carbon steel.

5) The residual stress parallel to the grinding direction is directed opposite to the horizontal direction of feed of the grinding wheel in the last pass.

6) Increasing depth of cut increases the residual normal stresses.

7) Cooling decreases the tensile residual stresses in a medium carbon steel, but increases them in Armco iron.

8) In steel (but less in iron) principal stresses in grinding are tilted around an axis transverse to the grinding direction.

9) Flattening a ground specimen does not change the residual shear stresses, although it alters the normal stresses.

ACKNOWLEDGEMENTS

This research was supported by ONR under Grant No. N00014-75-C-0580. The measurements were carried out in the Long-Term X-ray Facility of Northwestern University's Materials Research Center, supported in part by NSF through Grant No. DMR76-80847. One of us (H.D.) would like to thank the U.S. Fulbright-Hays Program for a travel grant.

We also thank the Institut fur Werkstoffkünde, T. H. Aachen, for preparing the samples.

REFERENCES

1. L. A. Glickman and V. A. Stepanov: J. Techn. Phys. USSR, 1946, Vol. 16, pp. 791-802.

2. J. Frisch and E. G. Thomsen: Trans. ASME, 1951, Vol. 73, pp. 337-46.

3. H. R. Letner: Trans. ASME, 1955, Vol. 77, pp. 1089-98.

4. L. V. Colwell, M. J. Sinnott and J. C. Tobin: Trans. ASME, 1955, Vol. 77, 1099-1105.

5. E. K. Henriksen: Tool Engineer, 1957, Vol. 38, 92-96.

6. D. P. Koistinen and R. E. Marburger: Trans. ASM, 1959, Vol. 51, pp. 537-55.

7. W. P. Koster, M. Field, L. J. Fritz, L. J. Gatto and J. R. Kahles: Rep. AFML-TR-70-11 to U.S. Air Force Materials Laboratory, Metcut Research Assoc., Inc., 1970.

8. E. Schreiber: Härterei-Techn. Mitt., 1973, Vol. 28, pp. 186-200.

9. P. S. Prevey: Adv. in X-ray Analysis, 1976, Vol. 19, pp. 709-24.

10. G. Faninger and H. Walburger: Härterei-Techn. Mitt., 1976, Vol. 31, pp. 79-82.

11. U. Wolfstieg and E. Macherauch: Härterei-Techn. Mitt., 1976, Vol. 31, pp. 83-85.

12. B. Syren, H. Wohlfahrt and E. Macherauch: Arch. Eisenhüttenwes, 1977, Vol. 48, 421-24.

13. D. F. Stein: Acta Met., 1966, Vol. 14, 99-104.

14. C. J. McMahon: "Microplastic Behaviour in Iron" in Adv. in Mater. Sci. Res., Vol. 2, 121-140, Interscience, New York, 1968.

15. C. W. Maschall and R. E. Marginer: "Dimensional Instability," Chapter 6, pp. 139-212, Pergamon-Press, Oxford-New York, 1977.

16. H. Dölle and V. Hauk: Härterei-Techn. Mitt, 1976, Vol. 31, pp. 165-168.

17. H. Dölle: J. Appl. Cryst, in print.

18. C. S. Barrett and T. B.Massalski: "Structure of Metals," 3rd ed., McGraw-Hill, New York, 1966.

19. B. D. Cullity: "Elements of X-ray Diffraction," Addison-Wesley, Reading, 1956.

20. M. R. James and J. B. Cohen: "The Measurement of Residual Stresses by X-ray Diffraction Techniques," In Experimental Methods of Materials Science, Vol. 1.

21. B. D. Cullity: J. Appl. Physics, 1964, Vol. 35, pp. 1915-17.

22. B. D. Cullity: Adv. in X-ray Analysis, 1977, Vol. 20, pp. 259-71.

23. A. Peiter: Härterei-Techn. Mitt., 1976, Vol. 31, pp. 158-64.

24. H. Dölle and V. Hauk: Z. Metallkde., 1977, Vol. 68, pp. 725-28.

25. H. Walburger: Conf. on Residual Stress Analysis, Starnberg, Germany, 1973.

26. E. Macherauch and U. Wolfstieg: J. Mater. Sci. and Eng., 1977, Vol. 30, pp. 1-13.

27. E. Christ and H. Krause: Z. Metallkde., 1975, Vol. 66, pp. 615-18.

28. H. Krause and H. H. Jühe: Wear, 1977, Vol. 36, pp. 15-21.

29. P. D. Evnschor and V. Hauk: Z. Metallkde., 1975, Vol. 66, pp. 167-68.

30. H. Dölle and V. Hauk: Härterei-Techn. Mitt., in print.

31. M. R. James and J. B. Cohen: Adv. in X-ray Analysis, 1977, Vol. 20, pp. 291-308.

32. G. Faninger, V. Hauk, E. Macherauch and U. Wolfstieg: Härterei-Techn. Mitt., 1976, Vol. 31, pp. 109-11.

33. F. Bollenrath, V. Hauk and E. H. Müller: Z. Metallkde., 1967, Vol. 58, 76-82.

34. H. Landolt-Börnstein, edit., K. -H. Hellwege, New Series, Group III: Crystal andSolid State Physics, Vol. 2, pp. 1-3, Springer-Verlag, Berlin-Heidelberg-New York, 1969.

35. E. Kröner, Z. Physik, 1958, Vol. 151, 504-518.

36. G. Faninger, Act. Phys. Austriaca, 1966, Vol. 24, pp. 245-70.

37. J. B. Cohen, H. Dolle and M. R. James: International Conference on Powder Diffraction, NBS, in press.

38. H. Neerfeld: Mitt. K. W. I. Eisenforsch. Düsseldorf, 1944, Vol. 27, pp. 81-89.

39. H. Dölle and V. Hauk: Z. Metallkde., 1978, Vol. 63, 410-17.

40. H. Krause and H. H. Jühe: Harterei-Techn. Mitt., 1976, Vol. 31, pp. 168-70.

41. N. Brown and R. A. Ekvall, Acta Met., 1962, Vol. 10, 1101-1107.

42. K. Kolb and E. Macherauch, Arch. Eisenhüttenwes., 1965, Vol. 36, 9-27.

43. F. Bollenrath, V. Hauk and W. Weidemann, Arch. Eisenhüttenwes., 1967, Vol. 38, 793-800.

44. A. S. Keh and S. Weissmann: In Electron Microscopy and Strength of Crystals (edit. G. Thomas and J. Washburn), pp. 231-300, Interscience, New York, 1963.

Table I. Composition of Steels in Weight Percent

	Armco-iron	Steel
C	0.02	0.57 - 0.65
Si	.....	0.15 - 0.35
Mn	0.08	0.60 - 0.30
S[max]	0.015	0.45
P[max]	0.02	0.45

Table II. Grinding Conditions for Each Sample

Samples	A1, C1°	A2, C2°	A3, C3°	A4, C4°	A5, C5°	A6, C6°
downfeed in μm	5	5	10	5	5	10
cooling	no	yes	yes	no	yes	yes
grinding direction	→	→	→	←	←	←

°A = Armco Iron
C = Steel

size of the grinding disk: ∅ 250 x 25 mm

grinding material: Corondum disk with a grain diameter of 600 μm

resolutions: 50 s^{-1}

table speed: 0.33 m s^{-1}

side feed: 0

grinding direction:
a) to the short head only (→), see Fig. 3
b) alternating, ending with grinding to the long head of the sample (←)

cooling
a) no cooling
b) cooling by water

Table III. Experimental Results for Specimen C5

strain components ϵ_{ij} in 10^{-4}	12.6	0.8	3.6
	0.8	7.8	$-.0_5$
	3.6	$-.0_5$	-4.5
stress components σ_{ij} in MPa	390	14	63
	14	306	-1
	63	-1	92
principal stresses σ_i and their directions $\underline{H}_i$ $(\varphi_i, \eta_i)^\circ$	σ_i	φ_i	η_i
	405	8.1	11.3
	304	97.6	-2.5
	79	175.3	78.3

°Angles defined in Fig. 8a.

Results when $\sin^2\psi$-method or two-tilt method is used

$\sin^2\psi$

$$\begin{pmatrix} 298 & 14 & 0 \\ 14 & 218 & 0 \\ 0 & 0 & 0 \end{pmatrix}$$ stresses in MPa

two-tilt $\psi = 0$ and 45°

$$\begin{pmatrix} 356 & 14 & 0 \\ 14 & 218 & 0 \\ 0 & 0 & 0 \end{pmatrix}$$ stresses in MPa

two-tilt $\psi = 0$ and -45°

$$\begin{pmatrix} 151 & 14 & 0 \\ 14 & 218 & 0 \\ 0 & 0 & 0 \end{pmatrix}$$ stresses in MPa

Table IV. Residual Stress Tensors (in MPa) for the Different Samples in Table II.°

specimen	Armco-iron			parameter of grinding	specimen	steel		
	151	-7	-7	n.c.		567	2	-65
A1:	-7	11	0	→	C1:	2	508	-4
	-7	0	28	5		-65	-1	137
	267	-12	-4	c		199	-10	-63
A2:	-12	367	8	→	C2:	-10	86	5
	-4	8	55	5		-63	5	84
	611	-8	9	c		541	-20	-38
A3:	-8	507	4	→	C3:	-20	565	1
	9	4	90	10		-38	1	86
	74	39	12	n.c.		408	-17	59
A4:	39	80	6	←	C4:	-17	416	6
	12	6	4	5		59	6	108
	380	16	18	c		390	14	63
A5:	16	351	9	←	C5:	14	306	-1
	18	5	-28	5		63	-1	92
	645	0	8	c		534	-2	69
A6:	0	557	8	←	C6:	-2	468	-3
	8	8	82	10		69	-3	95

°nc: no cooling

c: cooling

≠ : final grinding direction, $\pm \underline{P}_1$

5,10: downfeed in μm

FIGURE CAPTIONS

Fig. 1: Friction (F_t) and normal forces (F_n) acting on a specimen being ground and resolved stresses σ_{ij} related to the sample co-ordinate system (Fig. 2).

Fig. 2: Definition of Φ and Ψ and orientation of the laboratory system $\underline{L}_i$ with respect to the sample system $\underline{P}_i$. A positive Ψ tilt is shown. Grinding is in the $\underline{P}_1$-direction (positive for a single cutting direction, negative for the final pass when grinding alternately in two directions).

Fig. 3: Dimensions of the samples (in mm). The short head is defined as the positive $\underline{P}_1$-direction.

Fig. 4: Peak shifts due to displacement of the sample from the Ψ rotation axis.

Fig. 5: Peak shifts due to method of peak location vs. half-width of the peak.

Fig. 6: ϵ'_{33} vs. $\sin^2\Psi$ for sample C5.

Fig. 7: ϵ'_{33} ($\Phi = 0$) vs. $\sin^2\Psi$ for various samples showing the reversal of the position of the curves $\Psi > 0$, $\Psi < 0$, when the final grinding direction is reversed.

Fig. 8a: Definition of angles φ_i η_i used in Table III.

8b: Directions H_i of principal stresses σ_1 and σ_3 and the relationship between applied residual stresses σ^a_{13} and residual shear stresses σ^n_{13}.

Fig. 1 Friction (F_t) and normal forces (F_n) acting on a specimen being ground and resolved stresses σ_{ij} related to the sample co-ordinate system (Fig. 2).

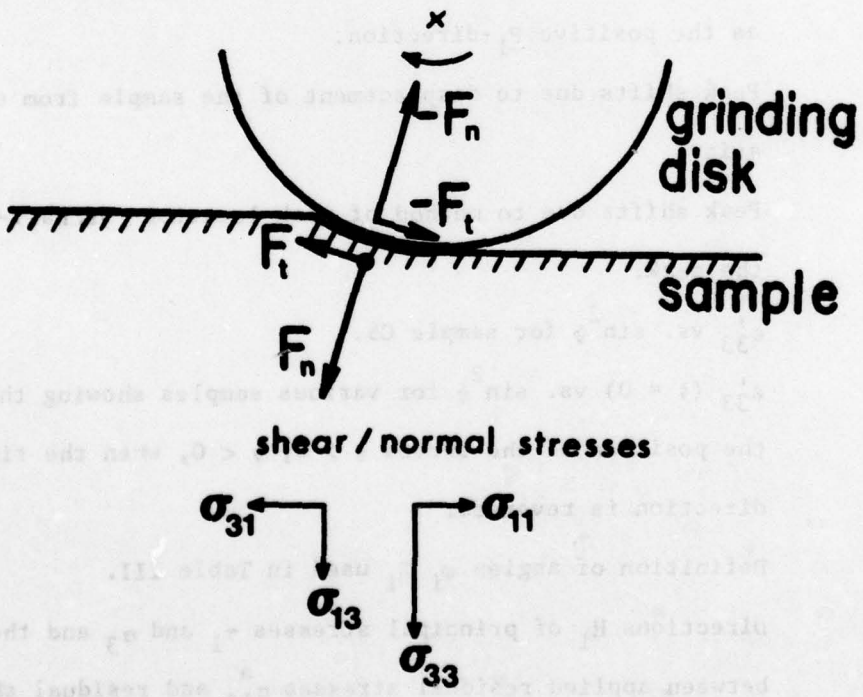

H. Dölle and J. B. Cohen fig. 1

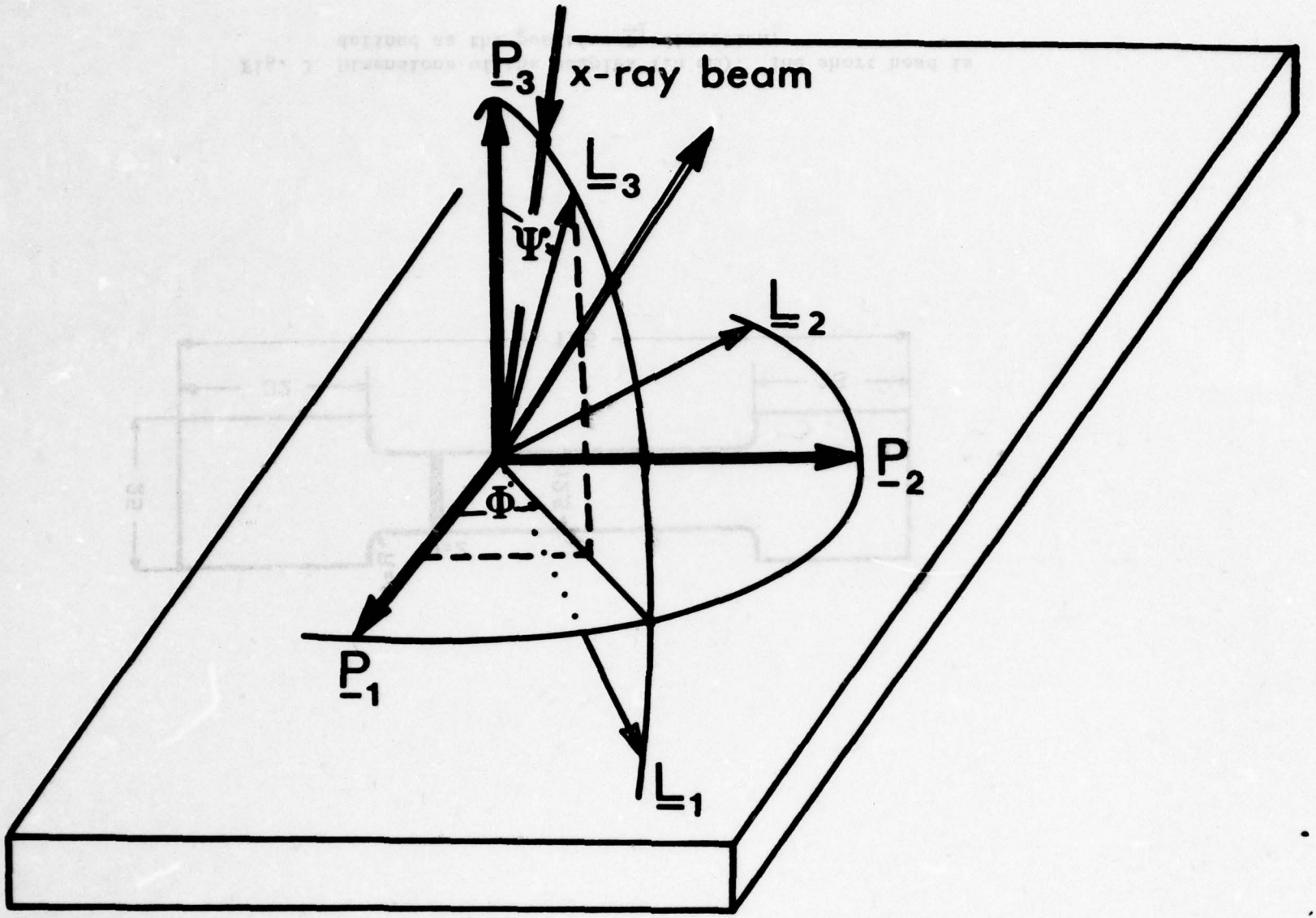

H. Dölle and J. B. Cohen

fig. 2

Fig. 2 Definition of ϕ and ψ and orientation of the laboratory system $\underline{L}_i$ with respect to the sample system $\underline{P}_i$. A positive ψ tilt is shown. Grinding is in the $\underline{P}_1$ direction (positive for a single

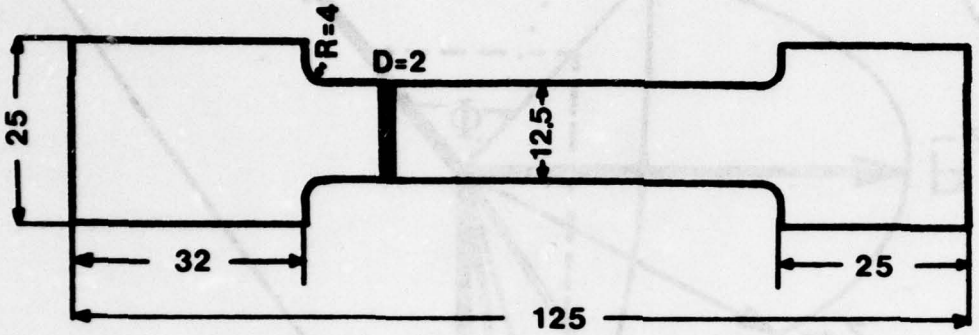

Fig. 3 Dimensions of the samples (in mm). The short head is defined as the positive $\underline{P}_1$-direction.

H. Dölle and J. B. Cohen fig.3

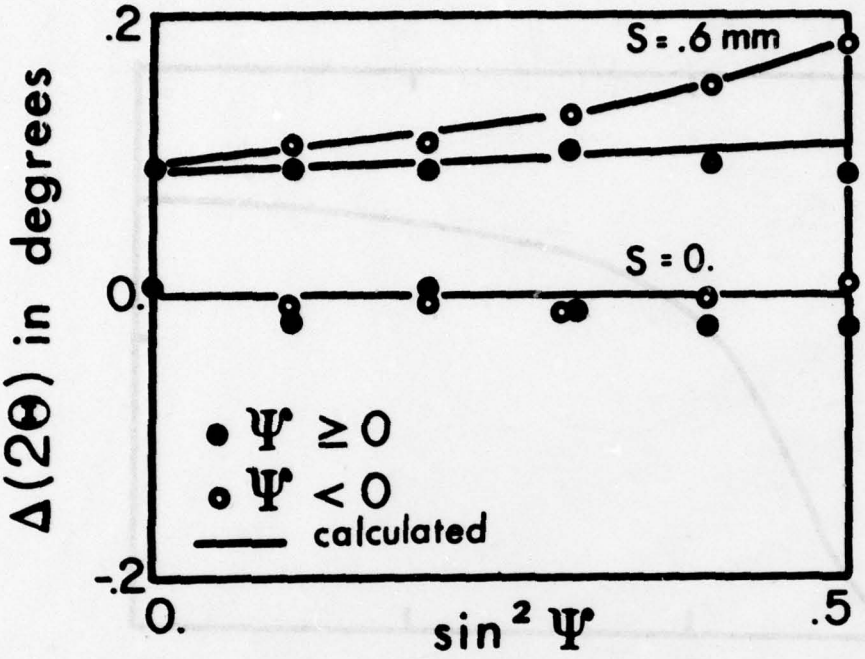

Fig. 4 Peak shifts due to displacement of the sample from the ψ rotation axis.

H. Dölle and J. B. Cohen

fig. 4

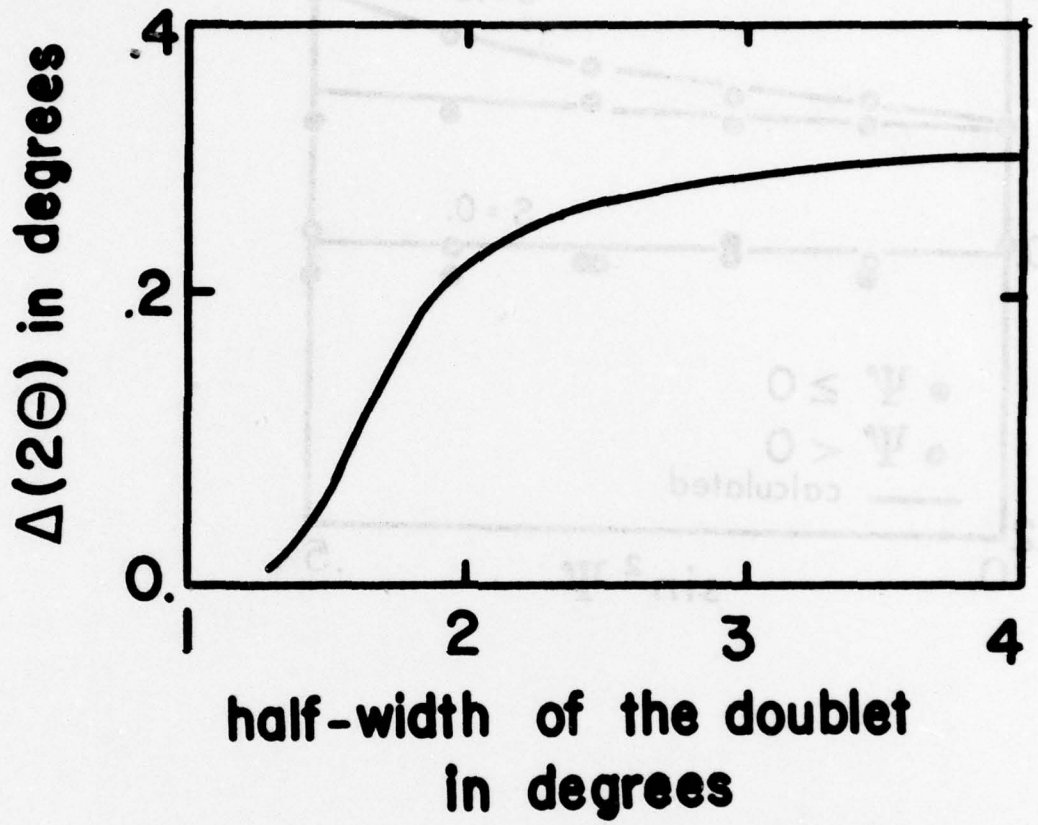

Fig. 5 Peak shifts due to method of peak location vs. half-width of the peak.

H. Dölle and
J. B. Cohen

fig. 5

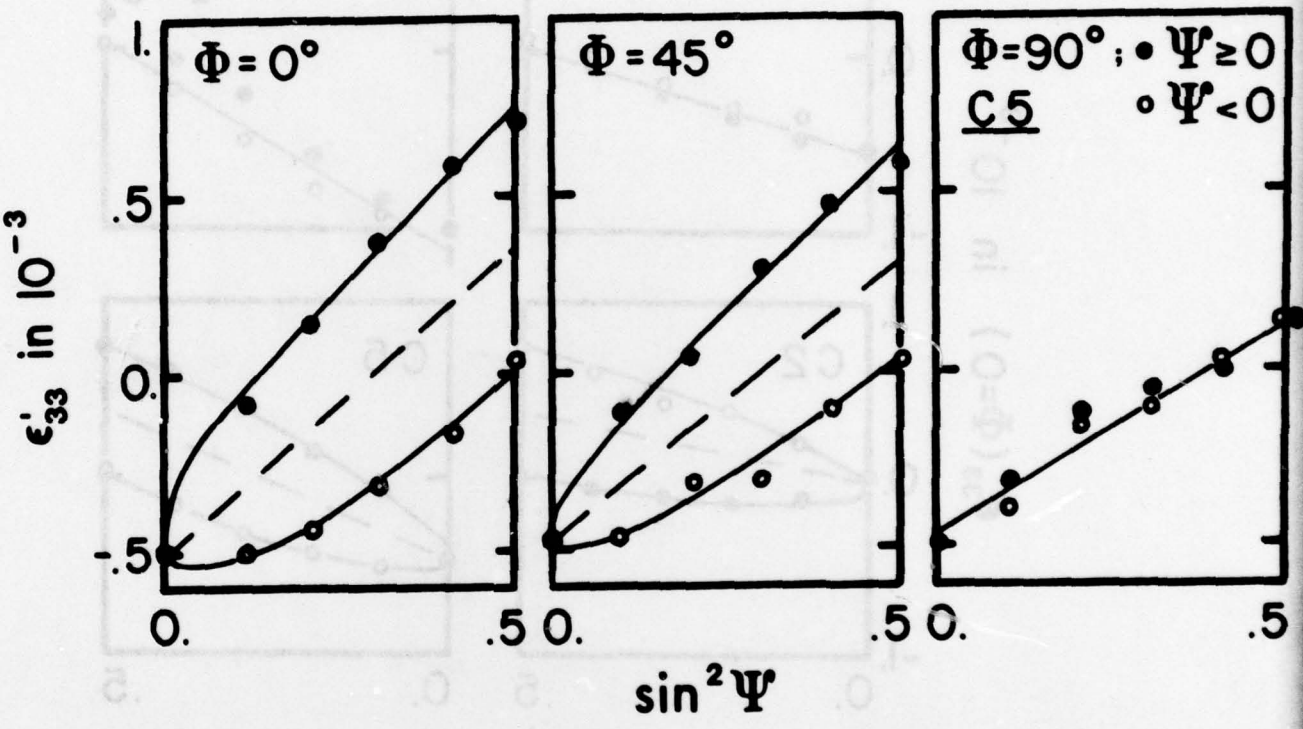

Fig. 6 ϵ'_{33} vs. $\sin^2\psi$ for sample C5.

H. Dölle and J. B. Cohen fig. 6

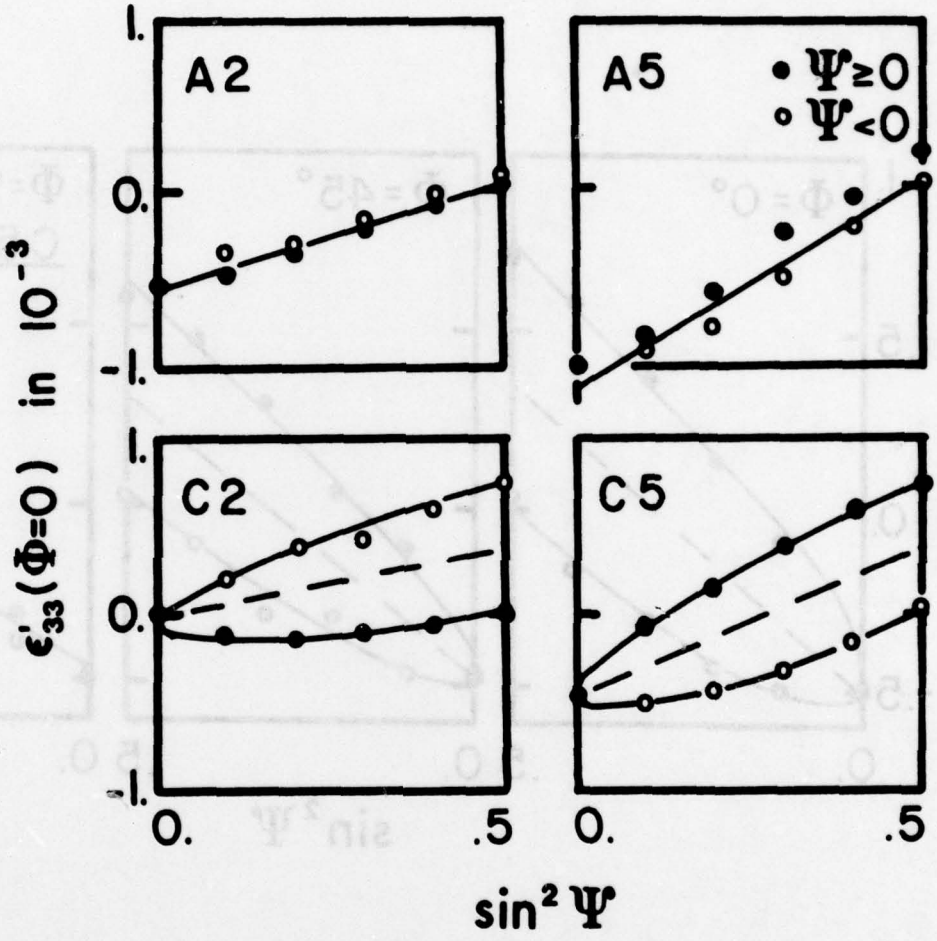

Fig. 7 ϵ'_{33} ($\phi = 0$) vs. $\sin^2\psi$ for various samples showing the reversal of the position of the curves $\psi > 0$, $\psi < 0$, when the final grinding direction is reversed.

H. Dölle and J. B. Cohen fig. 7

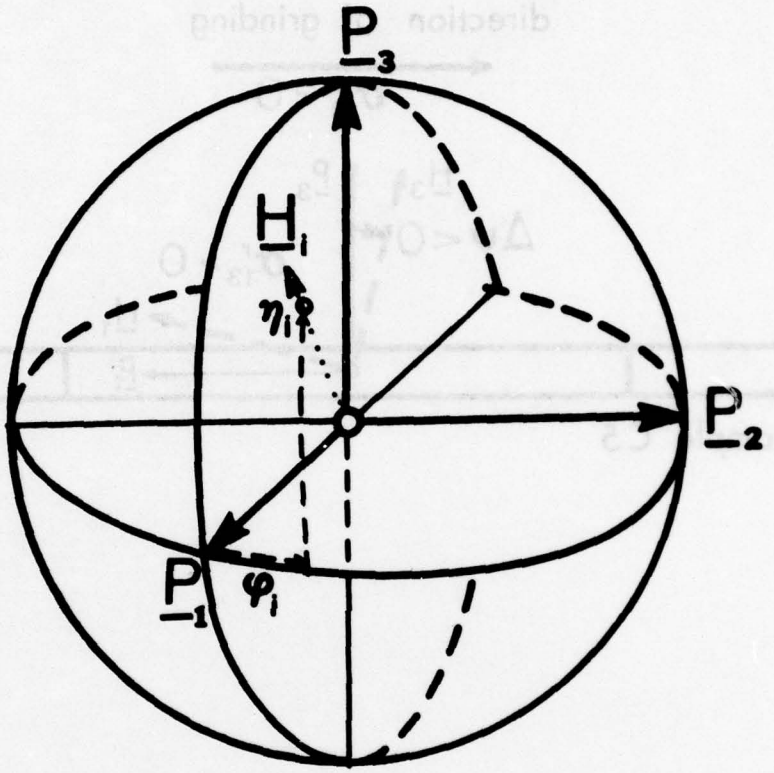

Fig. 8a Definition of angles φ_1 η_1 used in Table III.

H. Dölle & J. B. Cohen fig. 8a

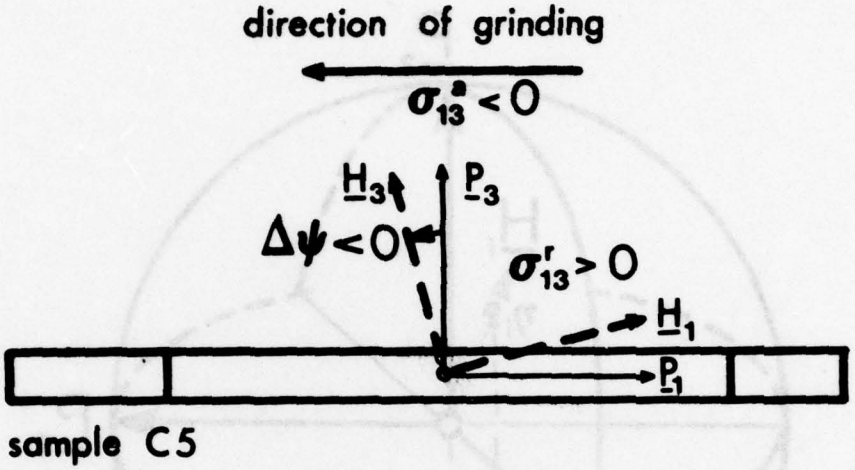

Fig 8b Directions H_i of principal stresses σ_1 and σ_3 and the relationship between applied residual stresses σ_{13}^a and residual shear stresses σ_{13}^n.

Security Classification

DOCUMENT CONTROL DATA - R & D

(Security classification of title, body of abstract and indexing annotation must be entered when the overall report is classified)

1. ORIGINATING ACTIVITY (Corporate author)

J. B. Cohen, Northwestern University
Evanston, Illinois 60201

2a. REPORT SECURITY CLASSIFICATION
unclassified

2b. GROUP

3. REPORT TITLE

RESIDUAL STRESSES IN GROUND STEELS

4. DESCRIPTIVE NOTES (Type of report and inclusive dates)
Technical Report No. 24

5. AUTHOR(S) (First name, middle initial, last name)

H. Dölle and J. B. Cohen

6. REPORT DATE
June 13, 1979

7a. TOTAL NO. OF PAGES
30 pages

7b. NO. OF REFS
44

8a. CONTRACT OR GRANT NO.
N00014-75-C-0580

b. PROJECT NO.
NR 031-733, Mod. No. P00005

c.

d.

9a. ORIGINATOR'S REPORT NUMBER(S)
24

9b. OTHER REPORT NO(S) (Any other numbers that may be assigned this report)

10. DISTRIBUTION STATEMENT

Distribution of this document is unlimited.

11. SUPPLEMENTARY NOTES

12. SPONSORING MILITARY ACTIVITY
Metallurgy Branch
Office of Naval Research

13. ABSTRACT

A new X-ray method for the evaluation of three dimensional (residual) stress states is demonstrated by studies of the effect of grinding on Armco-iron and a medium carbon steel. Although the penetration depth of the Cr-radiation employed in this study is only 5 μm, there is evidence of residual stresses normal to the surface (normal and shear components). In the past it has been assumed that these stress-components can be neglected. Shear stresses normal to the surface are small in Armco-iron, but significant ($\pm$ 60 MPa) in steel. From the sign of the shears, the direction of final grinding can be determined. Cooling decreases the tensile stresses parallel to the surface in steel; surprisingly, the opposite result is found in Armco-iron.

14. KEY WORDS	LINK A		LINK B		LINK C	
	ROLE	WT	ROLE	WT	ROLE	WT
grinding, machining, wear, residual stresses, stresses, X-rays, diffraction						